JTTEE5 5:269-276

Corrosion Fatigue Behavior of a Steel with Sprayed Coatings

K. Tokaji, T. Ogawa, J.U. Hwang, Y. Kobayashi, and Y. Harada

This paper describes the corrosion fatigue behavior and fracture mechanisms of a steel with different sprayed coatings. Rotating bending fatigue tests were conducted in 3% NaCl solution using specimens of a medium carbon steel with sprayed coatings of a ceramic (Cr_2O_3), a cermet (WC-12% Co) and two metals (Ni-11% P and Al-2% Zn). The corrosion fatigue process was basically the same for ceramic, cermet, and Ni-11% P sprayed specimens. That is, the corrosive media could be supplied from the specimen surface to the substrate through cracks initiated during fatigue cycling and/or pores in the coatings, and thus corrosion pits were generated followed by subsequent crack initiation and growth in the substrate.

The corrosion fatigue strength of ceramic sprayed specimens was slightly improved compared to that of the substrate steel because the under-coating (Ni-5% Al) could impede the penetration of the corrosive media although the ceramic coating had a poor resistance to cracking under cyclic loading. Cermet sprayed specimens also exhibited improved corrosion fatigue strength because of the high resistance to cracking and the low volume fraction of pores of the coating. In Ni-11% P sprayed specimens, cracks were initiated in the coating even at low stress levels; thus the corrosion fatigue strength was the same as that of the substrate. Anodic dissolution took place in Al-2% Zn coating because the coating was electrochemically poor, and thus the substrate was cathodically protected. Therefore, the corrosion fatigue strength of Al-2% Zn sprayed specimens was enhanced to as high as the fatigue strength of the substrate in room air.

Based on the experimental results, a dual-layer coating consisting of WC-12% Co and Al-2% Zn was fatigue tested. The coating was effective at low stress levels and exhibited long life under conditions where corrosion fatigue strength was critical.

Keywords ceramic coating, cermet coating, corrosion fatigue, dual-layer coating, fatigue strength, fracture mechanism, metal coating, NaCl solution, sprayed steel

1. Introduction

HARD COATINGS can enhance the resistance of metal alloys to wear, oxidation, thermal exposure, and corrosion. Of several surface coating techniques, thermal spraying has many advantages, such as applicability to materials of any shape and dimension, easy operation, and suitability for on-site application. Therefore, sprayed coatings of ceramics, cermets, metals, and plastics have been applied to various engineering fields, such as automobile, steelmaking, and energy industries. In such applications, sprayed components are often subjected to service conditions where fatigue strength is critical. However, the role of sprayed coatings on fatigue properties and the fracture mechanisms, in particular in corrosive environments, have not been studied in detail (Ref 1-4).

To investigate the corrosion fatigue behavior of a steel (medium carbon steel, S45C) with different sprayed coatings, rotating bending fatigue tests were conducted in a 3% NaCl solution. Four sprayed coatings with different mechanical and electrochemical properties were chosen: ceramic, cermet (WC-12%Co), Ni-11%P, and Al-2%Zn. The corrosion fatigue strength of sprayed steel was evaluated, and the fracture mechanisms are presented on the basis of detailed observation of crack initiation and growth on the longitudinal sections of the specimens. Based on the experimental results of each sprayed steel, a dual-layer coating was sprayed and fatigue tested.

K. Tokaji, T. Ogawa, and **J.U. Hwang,** Department of Mechanical Engineering, Gifu University, 1-1 Yanagido, Gifu 501-11, Japan; and **Y. Kobayashi** and **Y. Harada,** Thermal Spraying Technology R&D Laboratories, Tocalo Co., Ltd., Kobe 658, Japan.

2. Experimental Procedures

2.1 *Substrate*

The substrate material is a medium carbon steel (S45C) of chemical composition (wt%) 0.45C-0.21Si-75Mn-0.026P-0.013S-0.01Cu-0.02Ni-0.13Cr, balance Fe. The material with a diameter of 16 mm was heated up to 850 °C, held at this temperature for 1 h, and then tempered at 600°C for 1 h. Subsequently, tensile specimens (8 mm diameter, 80 mm gage length) and fatigue specimens (8 mm diameter, 10 mm gage length) were machined. Electropolished specimens of the substrate steel, denoted as EP, were used as a reference for the sprayed specimens.

2.2 *Sprayed Coatings*

Ceramic (Cr_2O_3), cermet (WC-12%Co), and two metals (Ni-11%P and Al-2%Zn), which have different mechanical and electrochemical properties, were the feedstock. The spray parameters for the ceramic coating are listed in Table 1. After being blasted with No. 46 white alumina at an air pressure of 0.31 MPa, Ni-5%Al and Cr_2O_3 were plasma sprayed as the undercoating and topcoating, respectively. As shown in Table 2, two different sprayed specimens were prepared, which were topcoating without the undercoating, denoted as TC, and undercoating plus the topcoating, denoted as TUC. For TUC

specimens, there are three different conditions of surface finish and thickness, t, of topcoating: TUC I, ground surface and t is 220 ± 20 μm; TUC II, ground surface and t is 400 ± 20 μm; and TUC III, as-sprayed surface and t is 250 ± 20 μm. TUCS specimens, which were subjected to a sealing treatment, were prepared from the TUC III specimens. Thermal setting polymer (DMC Superseal 21, Daiichi Meteco Co., Ltd., Tokyo, Japan) was used for the sealing treatment.

Table 3 represents the spray parameters for cermet and metal coatings. Cermet and Ni-11%P coatings were deposited by a high-velocity flame-spraying process after blasting with No. 60 white alumina at an air pressure of 0.4 MPa. The chemical compositions (wt%) of both powders were 12.0Co-1.0Fe, balance WC for cermet and 11.0P, <0.15C, balance Ni for the Ni-11%P material. A coating of Al-2%Zn was formed with a wire combustion process after blasting with No. 24 white alumina at an air pressure of 0.4 MPa. The chemical composition (wt%) of the wire was 0.14Si-0.003 Mn-0.18Fe-1.90Zn with the balance being Al. After being sprayed, the specimen surface was mechanically polished by diamond sheet (approximately No. 3000) for cermet sprayed specimens and by emery paper (approximately No. 2000) for Ni-11%P and Al-2%Zn sprayed specimens.

Table 4 gives the Vickers hardness, the volume fraction of pores and the adhesive strength of the coatings. The cermet coating exhibits a high adhesion strength. The ceramic coating is expected to have a high porosity, and the adhesion strength is 50 to 60 MPa (Ref 5).

2.3 *Experimental Procedures*

Fatigue tests were conducted using a 98 N · m capacity rotating bending fatigue testing machine at a loading frequency of 22.7 Hz, and additional experiments were performed at 2.5 Hz for Al-2%Zn sprayed specimens to study the effect of loading frequency. The observation of crack initiation and growth behavior was made on the longitudinal sections of the specimens using a light microscope and a scanning electron microscope (SEM).

The corrosive environment used is a 3% NaCl solution of 7.2 pH and a dissolved oxygen content of 7.82 ppm. The solution was led from a bath of 10 L capacity to the corrosion chamber through a temperature-controlled bath at 30 °C and was dripped onto the fatigue specimen at a rate of 10 cm^3/min. The solution was circulated between the bath and the chamber and was renewed every 15 days.

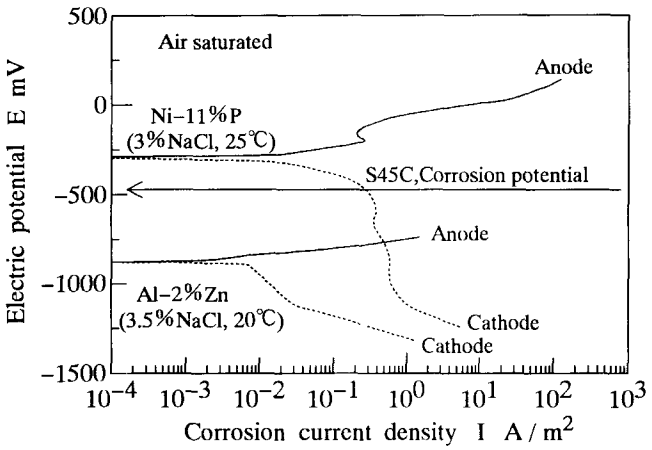

Fig. 1 Polarization curves for metal coatings

3. Results

3.1 *Electrochemical Properties of Coatings*

Before fatigue testing, the polarization curves were measured for Ni-11%P and Al-2%Zn coatings in 3% NaCl solution; see Fig. 1. The corrosion potential is higher for the Ni-11%P coating and lower for the Al-2%Zn coating compared to the free corrosion potential of the substrate steel, indicating that the former is electrochemically noble and the latter is less noble than the substrate.

3.2 *Tensile Properties*

The mechanical properties of sprayed specimens obtained from tensile tests are listed in Table 5, where the stresses were calculated using only the cross section area of the substrate.

Ceramic sprayed specimens with an as sprayed surface and a thickness of 380 ± 25 μm were employed for tensile tests. Results indicate that the ceramic coating has no influence on over-

Table 1 Plasma spray parameters for ceramic coating

Parameter	Undercoating	Topcoating
Material	Ni-5%Al	Cr_2O_3-5%SiO_2-3%TiO_2
Electric power of arc, kW	34	45
Plasma gas Ar, L/min	40	40
Plasma gas H_2, L/min	5	9
Powder size, μm	45 to ~106	15 to ~53
Distance, mm	130	100
Rotation of test specimen, rpm	500	500

Table 2 Specimen codes and preparation schedules for ceramic sprayed steel

Specimen code	Preparation schedule
TC	Topcoating without undercoating
TUC	Undercoating plus topcoating
TUC I	Ground surface and thickness, t, of 220 ± 20 μm
TUC II	Ground surface and thickness, t, of 400 ± 20 μm
TUC III	As-sprayed surface and thickness, t, of 250 ± 20 μm
TUCS	Sealing pores contained in TUC III specimens

Table 3 Spray parameters for cermet and metal coatings

Parameter	WC-12%Co	Ni-11%P	Al-2%Zn
Oxygen gas pressure, MPa	0.49 to ~0.64	0.59	0.25
Fuel gas	C_2H_2, C_3H_6	C_2H_2, C_3H_6	C_2H_2, C_3H_6
Fuel gas pressure, MPa	0.39 to ~0.49	0.44	0.11
Powder or wire size	10 to ~45 μm	10 to ~45 μm	3.2 mm
Distance, mm	150	200	150
Coating thickness, μm	120 ± 30	220 ± 30	120 ± 20
Process	Flame sprayed	Flame sprayed	Wire fuel

all strength. Surface observations revealed that many circumferential cracks perpendicular to the specimen axis were initiated at the early stage of loading far below the yield strength. For cermet and Al-2%Zn sprayed specimens, the lower yield point, σ_{yl}, did not appear, but Ni-11%P sprayed specimens exhibited distinct yielding phenomenon. In cermet sprayed specimens, cracks were initiated after reaching the upper yield point, σ_{yu}. The number of cracks increased with increasing deformation, and the coating peeled from the substrate before reaching the tensile strength, σ_{UTS}. Therefore, the σ_{yu} value becomes higher than that of the EP specimens because the coating can sustain loading, and the σ_{UTS} value is almost the same as that of the EP specimens. The Ni-11%P coating peeled from the substrate without any cracking just after reaching σ_{yu}, indicating the low adhesive strength of the coating (see Table 4). Thus, the σ_{yu} value is higher than for the EP specimens, and the σ_{yl} and σ_{UTS} values are consistent with those of the EP specimens. The Al-2%Zn coating is very soft; thus it has little effect on the mechanical properties. The σ_{yu} and σ_{UTS} values are the same as those of the EP specimens.

Table 4 Characteristics of cermet and metal coatings

Coating	Vickers hardness, HV	Porosity, %	Adhesive strength, MPa
WC-12%Co	1113	<0.5	150
Ni-11%P	488	<0.1	40 to ~59
Al-2%Zn	39	<10	20 to ~40

3.3 *Fatigue Strength*

The *S-N* diagrams for sprayed steel with different coatings are represented in Fig. 2 to 5, where the stress amplitudes, σ_s, were calculated using the substrate specimen diameter, that is, excluding the coating thickness.

3.3.1 Ceramic Sprayed Specimens

As shown in Fig. 2, the fatigue strengths in room air are almost the same for TC, TUC I, and TUC II; thus corrosion fatigue tests were conducted using TUC III and TUCS specimens. Details of the fatigue behavior in room air are provided elsewhere (Ref 6). The fatigue strengths of TUC III and TUCS specimens in 3% NaCl solution decrease markedly when compared to those of TC, TUC I, and TUC II specimens in room air. They were slightly higher than that of EP specimens, indicating that the ceramic coating marginally improves the corrosion fatigue strength. Figure 2 also shows that the corrosion fatigue strength of TUCS specimens is almost identical to that of TUC III specimens in the region of fatigue life, N_f, of less than 10^7 cycles; thus the sealing treatment seems to be ineffective in that region.

3.3.2 Cermet Sprayed Specimens

As shown in Fig. 3, the fatigue strength of cermet sprayed specimens in room air is significantly higher than that of EP specimens. The coating that has a high adhesive strength can en-

Table 5 Mechanical properties of sprayed specimens

Coating	Upper yield point (σ_{yu}), MPa	Lower yield point (σ_{yl}), MPa	Tensile strength (σ_{UTS}), MPa	Elongation (δ), %	Reduction of area (φ), %
EP	676	666	771	14	62
Cr_2O_3	677	671	761	13	71
WC-12%Co	709	...	767	...	66
Ni-11%P	701	647	754	..	70
Al-2%Zn	669	...	779	12	61

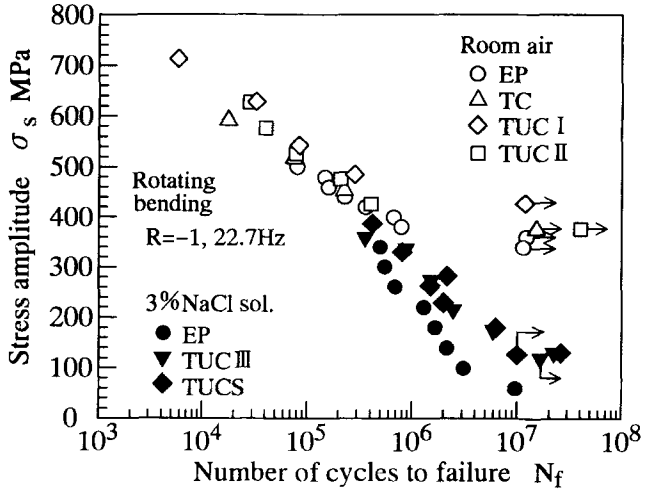

Fig. 2 *S-N* diagram for ceramic (Cr_2O_3) sprayed specimens. *R* is the stress ratio.

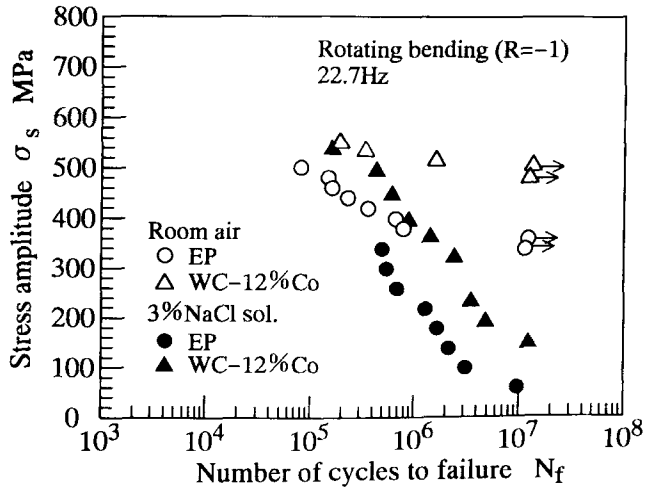

Fig. 3 *S-N* diagram for cermet (WC-12%Co) sprayed specimens. *R* is the stress ratio.

hance the crack initiation resistance of the substrate steel. On the other hand, the corrosion fatigue strength decreases, especially under high cycle regimes. However, when compared to EP specimens, the corrosion fatigue strength is clearly improved.

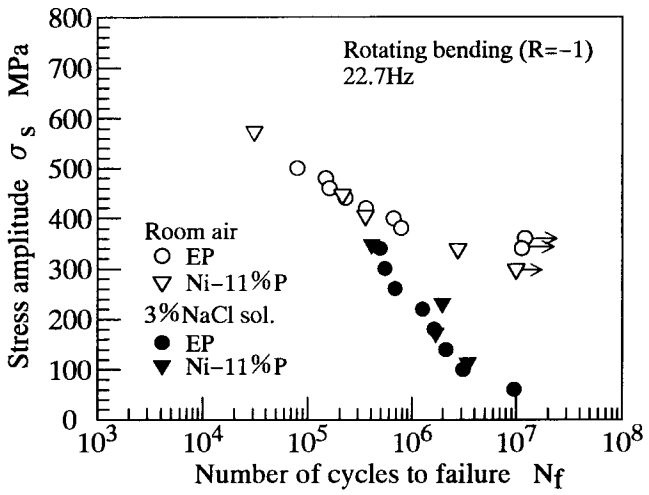

Fig. 4 *S-N* diagram for Ni-11%P sprayed specimens. *R* is the stress ratio.

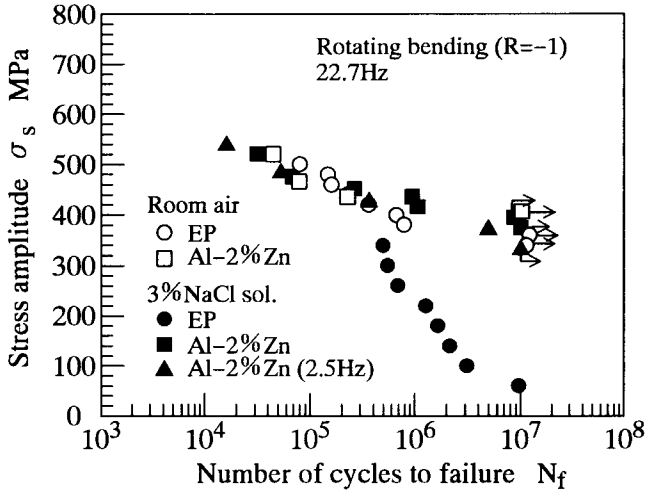

Fig. 5 *S-N* diagram for Al-2%Zn sprayed specimens. *R* is the stress ratio.

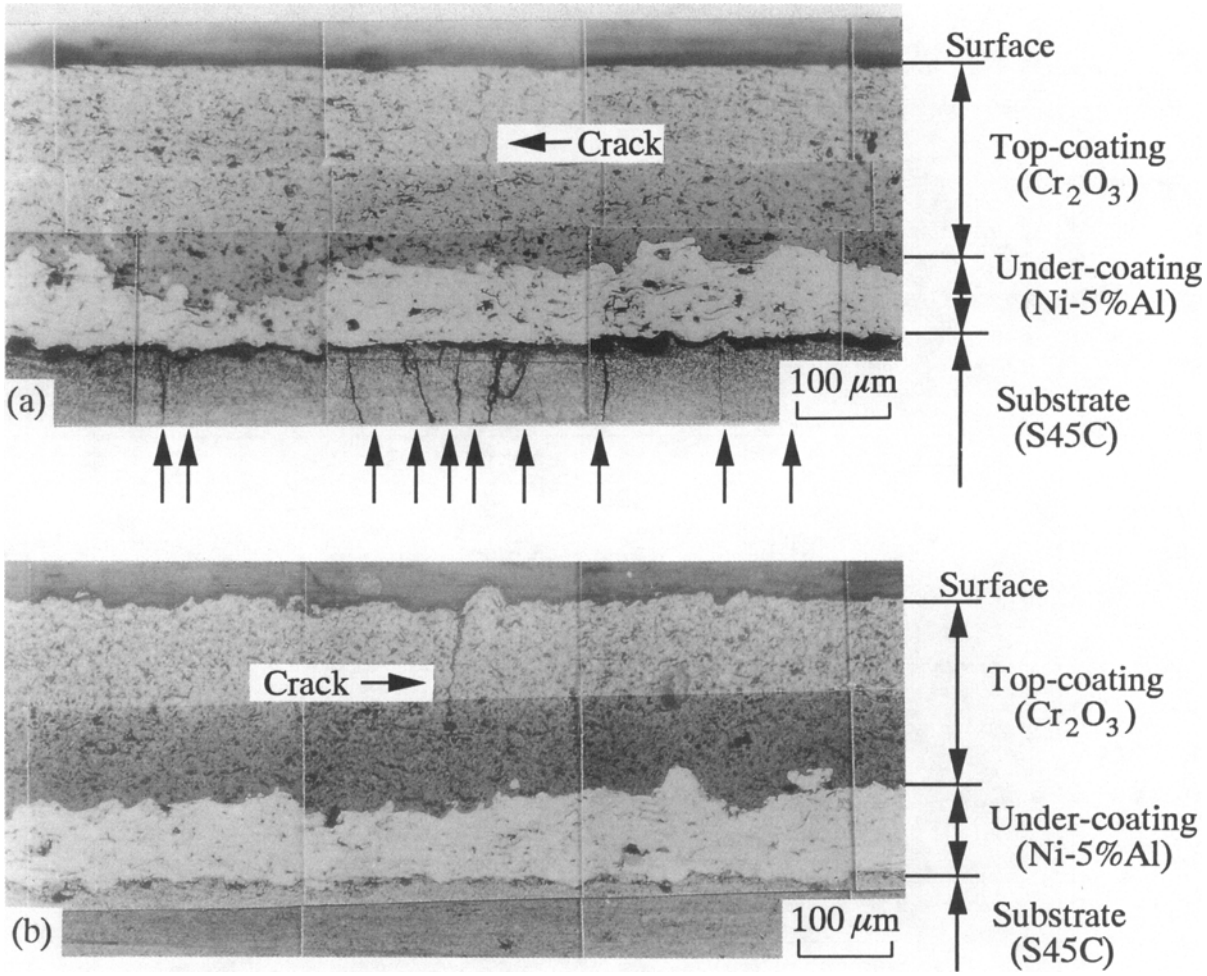

Fig. 6 Micrographs showing longitudinal sections of (a) TUC III and (b) TUCS specimens that were unbroken at N of 10^7 cycles in 3% NaCl solution at σ_S of 100 MPa

3.3.3 Ni-11% P Sprayed Specimens

The fatigue strengths of Ni-11%P sprayed specimens in room air and in 3% NaCl solution are the same as those of the EP specimens (see Fig. 4), indicating that the coating has no influence on fatigue strength in both environments. Cracks were observed in the coating of a specimen unbroken at fatigue life, N, of 10^7 cycles in room air, but they did not grow into the substrate because of coating delamination at the interface. In 3% NaCl solution, no appreciable corrosion was evident on the coating, but some rust exuded from cracks in the coating. This indicates that a corrosion reaction has occurred at the interface between the coating and the substrate.

3.3.4 Al-2% Zn Sprayed Specimens

The fatigue strength of Al-2%Zn sprayed specimens under ambient conditions is the same as that of EP specimens (see Fig. 5), showing that the soft coating has no contribution in improving fatigue strength. On the other hand, the fatigue strength in 3% NaCl solution is significantly improved to as high as that of the substrate under ambient conditions. Furthermore, the corrosion fatigue strength is not affected by loading frequency. At 2.5 Hz, however, corrosion dissolution was observed in the coating, which was revealed when it partially peeled from the substrate.

3.4 *Observation of Fatigue Cracks*

Longitudinal sections are shown in Fig. 6 for TUC III and TUCS specimens unbroken at N of 10^7 cycles at σ_s of 100 MPa in 3% NaCl solution. The observations were made near the crack initiation site in the topcoating. Arrows indicate cracks in the substrate. In the TUC III specimen, many cracks are observed in the substrate, which are localized near the site where a crack initiated in the topcoating. Some cracks are seen at locations away from the crack in the topcoating. On the other hand, in the TUCS specimen, no crack was observed in the substrate. Although there was no significant difference in fatigue lives between TUC III and TUCS specimens, as shown in Fig. 2, this observation suggests that a sealing treatment would improve the corrosion fatigue strength of sprayed steel in the N of greater than 10^7 cycles region.

Fatigue cycling was interrupted, and the interface between the undercoating and the substrate was examined by electron probe microanalysis (EPMA); see Fig. 7. Increased intensities of Na and Cl signals are detected at the interface, indicating that the solution was supplied to the interface from the specimen surface.

The specimen surface of a cermet sprayed specimen was periodically observed using a replication technique during fatigue cycling. No cracking initiated until just before failure, suggesting that the coating has an excellent resistance to cracking under cyclic loading. The section appearances are shown in Fig. 8 for a cermet sprayed specimen tested in 3% NaCl solution at a σ_s of 193 MPa, which was broken at N_f of 1.2×10^7 cycles. The coating peeled from the specimen surface over a length of several millimeters. Figure 8(a) shows the region where the coating completely peeled, and (b) shows the region where it is still attached to the substrate. As shown in Fig. 8(a), there are many cracks, which were initiated from corrosion pits generated at the substrate. Cracks are also observed in the substrate at locations where the coating is attached, but no cracks exist in the coating, see Fig. 8(b).

Figure 9 shows the section appearances for a Ni-11%P sprayed specimen tested in 3% NaCl solution at a σ_s of 113 MPa, which was broken at N_f of 3.4×10^6 cycles. As shown, a crack exists in the coating. The crack growth changes to the direction along the interface; that is, the crack does not grow continuously

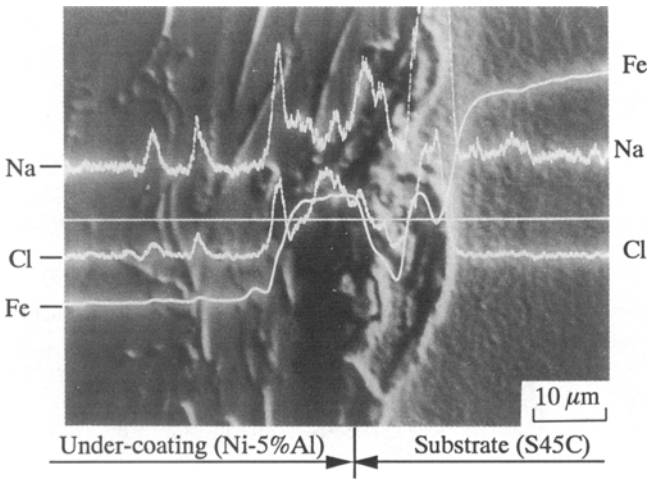

Fig. 7 EPMA analysis for a TUC III specimen showing the intensities of Fe, Na, and Cl signals, which indicates the penetration of the solution into the substrate

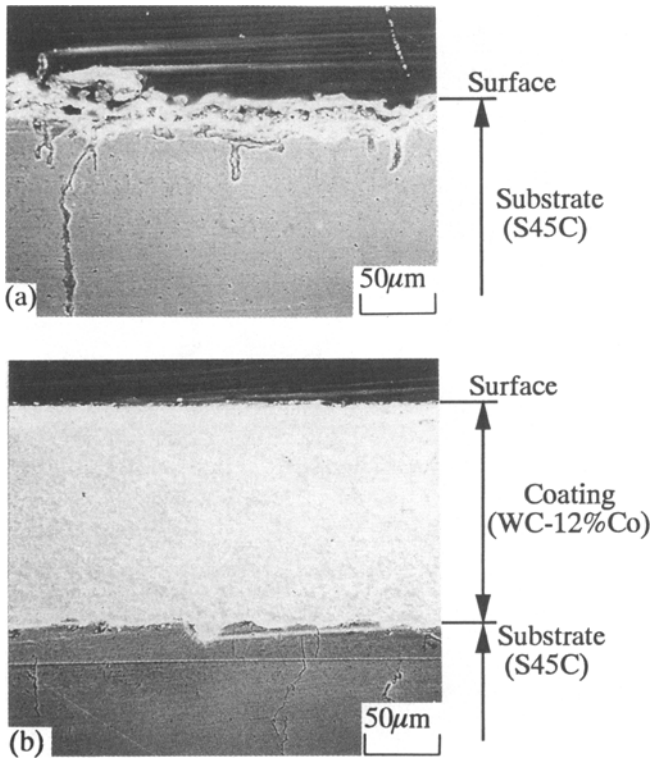

Fig. 8 Appearances of the longitudinal section of a broken WC-12%Co specimen at σ_s of 193 MPa, and N_f of 1.2×10^7 cycles. (a) Region where the coating peeled completely. (b) Region where the coating is still attached

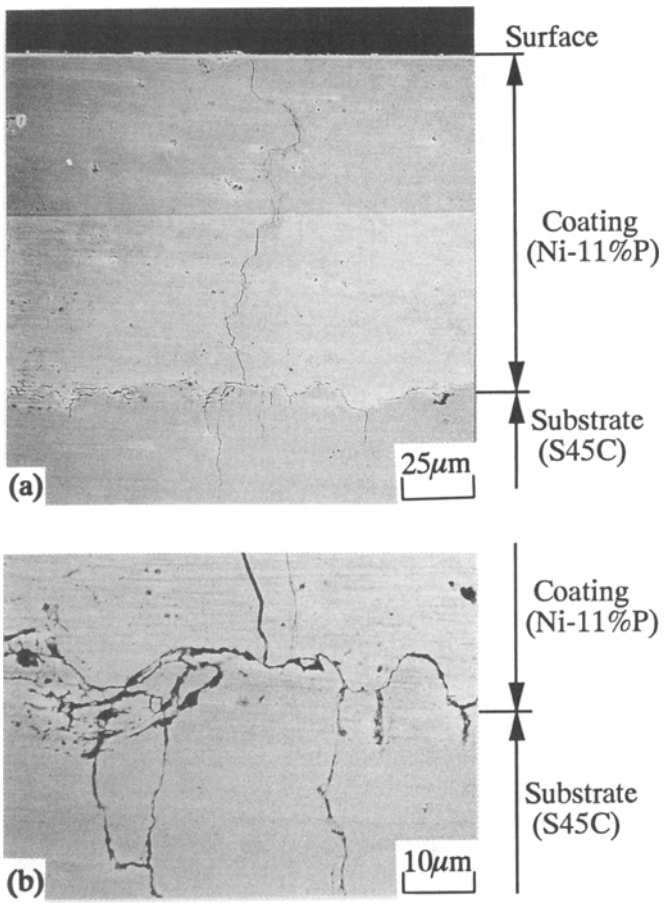

Fig. 9 Appearances of the longitudinal section of a broken Ni-11%P specimen at σ_s of 113 MPa and N_f of 3.4×10^6 cycles. (a) Micrograph showing cracks initiated in the coating and the substrate. (b) Magnified view of (a)

into the substrate because of delamination of the interface. The corroding solution can be supplied to the substrate through such cracks followed by the generation of corrosion pits and crack growth in the substrate.

Figure 10 shows the section appearance for an Al-2%Zn sprayed specimen tested in 3% NaCl solution at σ_s of 374 MPa, which was unbroken at N of 10^7 cycles. As shown in Table 4, the coating has a porosity of ~10%. Thus, the solution can be easily supplied to the interface through pores. Since the coating is less noble than the substrate (see Fig. 1), anodic dissolution takes place in the coating, and the substrate is cathodically protected. Therefore, corrosion pits and cracks are not observed in the substrate.

4. Discussion

4.1 *Corrosion Fatigue Mechanisms*

Fracture mechanisms are essentially the same for ceramic, cermet, and Ni-11%P sprayed steels. The corrosion fatigue process, which is illustrated schematically in Fig. 11, is considered as follows. (1) The corrosive media can be supplied to the surface of the substrate through cracks initiated during fatigue

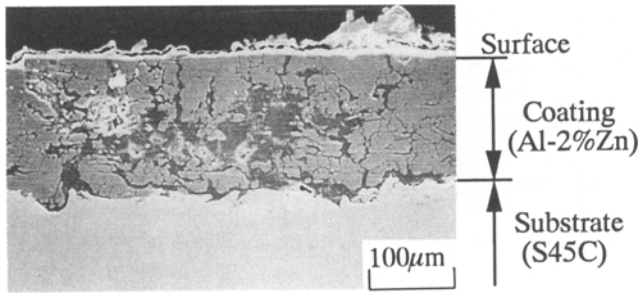

Fig. 10 Appearance of the longitudinal section of an unbroken Al-2%Zn specimen at σ_s of 374 MPa and N_f of $>1.0 \times 10^7$ cycles

cycling and/or pores contained in the coating. (2) Corrosion pits are generated on the substrate steel, which is electrochemically less noble, and subsequently, the adjacent interface delaminates. (3) Cracks are initiated from the corrosion pits and grow. (4) The specimen fails, and the coating near the fracture surface delaminates. The transportation of corrosive media is the controlling mechanism in the corrosion fatigue of sprayed steels. For those sprayed steels, factors influencing the corrosion fatigue strength are the resistance to cracking under cyclic loading, the volume fraction of pores, and the adhesive strength of the coatings.

In ceramic sprayed steel, cracks are initiated in the topcoating when stress levels are high because it has a poor resistance to cracking under cyclic loading. Also, the coating contains many pores; thus the solution can be supplied through cracks and/or pores. However, the undercoating (Ni-5%Al) impedes penetration of the corrosive media leading to a slightly improved corrosion fatigue strength. When the coating is subjected to a sealing treatment, the solution is supplied only from cracks in the topcoating. Therefore, at lower stress levels, when cracks are not initiated, the corrosion fatigue strength would be improved by a sealing treatment. The cermet coating has a high resistance to cracking, high adhesive strength, and low volume fraction of pores. Also, cracks were not initiated in the coating until just before failure. Therefore, the corrosive media is transported only through pores and needs more time to penetrate to the substrate. Thus, the corrosion fatigue strength can be improved. On the other hand, Ni-11%P coating has a poor resistance to cracking and low adhesive strength. Cracks are initiated easily in the coating at the early stage of fatigue cycling. The corrosive media can be supplied through such cracks. As a result, the corrosion fatigue strength of Ni-11%P sprayed steel was the same as that of the substrate steel.

Sprayed coatings inevitably contain many pores; thus even though no crackings are initiated during fatigue cycling, corrosion of the substrate steel cannot be avoided. However, to improve the corrosion fatigue strength of metal-sprayed steels, a method in which the coating is used as a sacrifice electrode is considered to be very effective as shown by the results of Al-2%Zn sprayed steel. As shown in Fig. 5, the corrosion fatigue strength was enhanced up to the strength of the substrate in room air. On the other hand, the anodic dissolution of the coating begins at the interface and proceeds to the interior of the coating. Consequently, the coating is filled up with corrosion products of low strength; thus the coating could peel easily. As shown in Fig. 5, the corrosion fatigue strength at 22.7 Hz was almost the same as that at 2.5 Hz in the N region of less than 10^7 cycles. However,

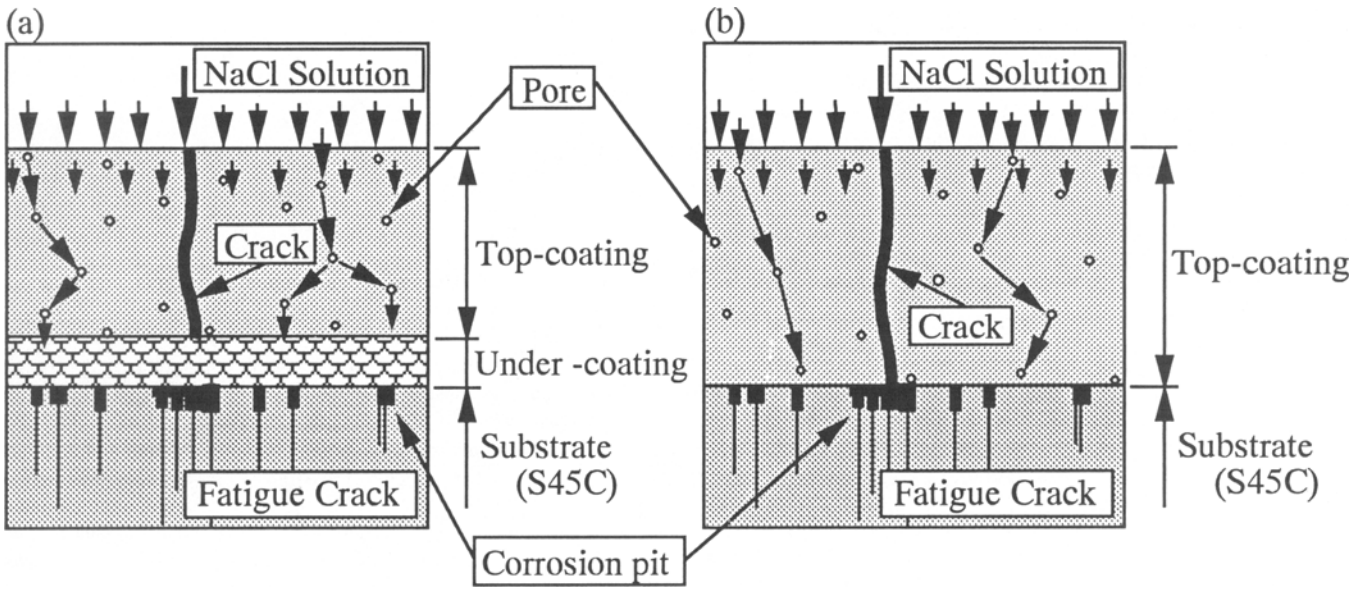

Fig. 11 Schematic illustrations of corrosion fatigue process (a) Ceramic (Cr_2O_3) sprayed steel. (b) Cermet (WC-12%Co) and Ni-11%P sprayed steels

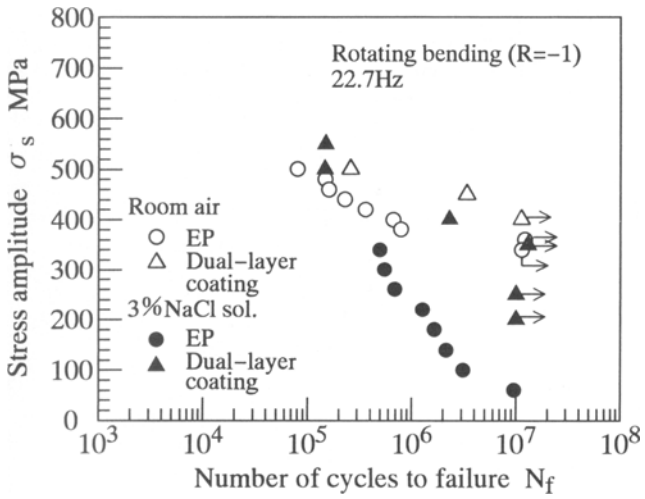

Fig. 12 *S-N* diagram for dual-layer coated specimens. *R* is the stress ratio.

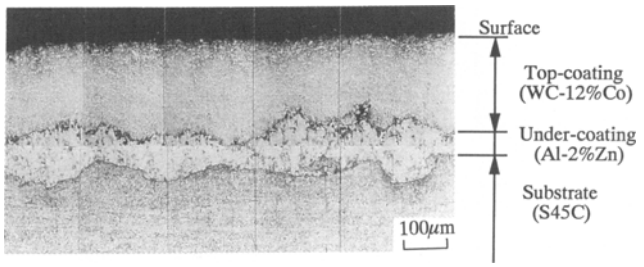

Fig. 13 Appearance of the longitudinal section of sprayed specimen with dual-layer coating unbroken at *N* of 10^7 cycles at σ_s of 200 MPa in 3% NaCl solution

in the longer life regime or at lower loading frequencies, the corrosion dissolution of the coating takes place much more severely, and thus it peels from the substrate. If the coating peels completely, then the effectiveness of the coating would be lost.

4.2 *Dual-Layer Coating*

Based on the experimental results of each sprayed steel, a dual-layer coating consisting of WC-12%Co and Al-2%Zn was considered, and sprayed specimens with the dual-layer coating were fatigue tested where WC-12%Co with the thickness of 165 ± 15 μm was used as topcoating and Al-2%Zn with the thickness of 115 ± 30 μm was employed as an undercoating. The *S-N* diagram is shown in Fig. 12. The fatigue strength in 3% NaCl solution is almost the same as that of the EP specimens under ambient conditions indicating improved corrosion fatigue strength equivalent to the Al-2%Zn sprayed specimens. However, at σ_s of 350 MPa, cracks were observed in the coating for the specimen unbroken at *N* of 10^7 cycles. Cracks were also noticed at σ_s of 250 MPa, but no cracks were initiated at σ_s of 200 MPa.

A longitudinal section of a specimen unbroken at *N* of 10^7 cycles at σ_s of 200 MPa, Fig. 13, shows no corrosion or damage in the coating and the substrate. Therefore, the proposed dual-layer coating is effective at lower stress levels or under longer life regimes where corrosion fatigue strength is critical.

5. Conclusions

In the present study, rotating bending fatigue tests were conducted in 3% NaCl solution using specimens of a medium carbon steel (S45C) with sprayed coatings of a ceramic (Cr_2O_3), a cermet (WC-12%Co), and two metals (Ni-11%P and Al-2%Zn), and the corrosion fatigue strength and fracture mechanisms were investigated. The conclusions obtained are summarized as follows.

- The corrosion fatigue strength of ceramic sprayed steel was slightly higher than that of the substrate steel. A sealing treatment had little effect on improving the corrosion fatigue strength at higher stress levels because many cracks were initiated in the topcoating. It could be effective in long life regions of more than 10^7 cycles.
- The corrosion fatigue strength of WC-12%Co sprayed steel was improved compared to that of the substrate steel because of the high resistance to cracking and the low porosity of the coating.
- In Ni-11%P sprayed steel, cracks were readily initiated in the coating at the early stage of fatigue cycling. Therefore, the corrosion fatigue strength was the same as that of the substrate steel because the corrosive media could be supplied to the substrate through cracks and pores.
- Anodic dissolution took place in Al-2%Zn coatings, and no corrosion occurred in the substrate because the coating was less noble than the substrate steel. Consequently, the corrosion fatigue strength of Al-2%Zn sprayed steel was improved to levels equivalent to the substrate under ambient conditions.
- Based on the experimental results, a dual-layer coating of WC-12%Co and Al-2%Zn was sprayed and fatigue tested. The coating was effective at lower stress levels in the long life regimes where corrosion fatigue strength was critical.

Acknowledgments

The authors wish to thank Mr. T. Ejima for assistance with the experiments.

References

1. S.L. Evans and P.J. Gregson, The Effect of a Plasma-Sprayed Hydroxyapatite Coating on the Fatigue Properties of Ti-6Al-4V, *Mater. Lett.*, Vol 16 (No. 5), 1993, p 270-274
2. H. Nakahira, Y. Harada, K. Tani, R. Ebara, and Y. Yamada, Improvement of Corrosion Fatigue Strength of High Strength Steel by Thermal-Sprayed (WC-Cr-Ni) Cermet Coating, *J. Soc. Mater. Sci., Jpn.*, Vol 43 (No. 490), 1994, p 888-894 (in Japanese)
3. M. Sugano, H. Masaki, J. Kishimoto, Y. Nasu, and T. Satake, A Microstructural Study of Fatigue Damage in Stainless Steel Coated with Plasma-Sprayed Alumina, *Thermal Spraying: Current Status and Future Trends*, A. Ohmori, Ed., High Temperature Society of Japan, 1995, p 145-150
4. T. Shiraishi, H. Ogiyama, and H. Tsukuda, Effect of Thermal Sprayed Ceramic Coatings on Fatigue Behavior of Metals, *Thermal Spraying: Current Status and Future Trends*, A. Ohmori, Ed., High Temperature Society of Japan, 1995, p 845-850
5. The Japan Society of Precision Engineering, Plasma Spraying, *Hyomenkaishitsugijutsu*, The Nikkan Kogyo Shimbun, 1988, p 182 (in Japanese)
6. J.U. Hwang, T. Ogawa, and K Tokaji, Fatigue Strength and Fracture Mechanisms of Ceramic-Sprayed Steel in Air and a Corrosive Environment, *Fatigue Fract. Eng. Mater. Struct.*, Vol 17 (No. 7), 1994, p 839-848